IEEE TRANSACTIONS ON
PLASMA
SCIENCE

IEEE Xplore Digital Library
http://ieeexplore.ieee.org/Xplore

Symplectic Maps for Diverted Plasmas

Iberê L. Caldas, Bruno F. Bartoloni, David Ciro, Geraldo Roberson, Adriane B. Schelin, Tiago Kroetz, Marisa Roberto, Ricardo L. Viana, Kelly C. Iarosz, Antonio M. Batista, Philip J. Morrison

***Abstract*—Nowadays, divertors are used in the main tokamaks to control the magnetic field and to improve the plasma confinement. In this article, we present analytical symplectic maps describing Poincaré maps of the magnetic field lines in confined plasmas with a single null poloidal divertor. Initially, we present a divertor map and the tokamap for a diverted configuration. We also introduce the Ullmann map for a diverted plasma, whose control parameters are determined from tokamak experiments. Finally, an explicit, area-preserving and integrable magnetic field line map for a single-null divertor tokamak is obtained using a trajectory integration method to represent toroidal equilibrium magnetic surfaces. In this method, we also give examples of onset of chaotic field lines at the plasma edge due to resonant perturbations.**

***Index Terms*—magnetic surfaces, symplectic map, divertor.**

I. Introduction

TOKAMAKS are the most promising devices to confine fusion plasmas [1], [2]. The plasma confinement depends on the magnetic field which determines the particle transport [3]. To the leading order approximation, the charged particles follow the magnetic field lines [2], [3]. Thus, the particle transport can be controlled by properly modifying the magnetic field as a result of electrical currents in external coils and also by installing poloidal divertors [1], [4]. Such divertors are used to control the plasma impurity content [5], [6] and have a special magnetic configuration created by electric currents in external coils, such that the field lines have escape channels, through which plasma particles can be diverted out of the tokamak wall and redirected to divertor plates.

Divertors are essential components in modern tokamaks, such as ITER [1], [7]. The overlap of the magnetic fields created by the divertor with the magnetic field of the plasma creates a hyperbolic fixed point where the poloidal magnetic field is null. The hyperbolic point is in the separatrix, the invariant line separating the plasma, with stable and unstable manifolds [8], [9]. Outside the separatrix the magnetic field lines intersect the collector plates [1].

I. L. Caldas and K. C. Iarosz are with the Institute of Physics at University of São Paulo, Brazil. E-mail:ibere@if.usp.br

B. Bartoloni is with the Departamento de Ensino Geral at Faculdade de Tecnologia de São Paulo, São Paulo, Brazil.

D. Ciro and R. L. Viana are with the Department of Physics at Federal University of Paraná, Curitiba, Brazil.

G. Roberson and M. Roberto are with the Aeronautics Institute of Technology at CTA, São José dos Campos, Brazil.

A. Schelin is with the Institute of Physics at University of Brasília, Brasília, Brazil.

T. Kroetz is with the Department of Mathematics at Federal Technological University of Paraná, Pato Branco, Brazil.

A. M. Batista is with the Department of Mathematics and Statistics at State University of Ponta Grossa, Ponta Grossa, Brazil.

P. J. Morrison is with the Institute for Fusion Studies at The University of Texas at Austin, USA.

$978-1-5386-3386-1/17/\$31.00f$

Digital Object Identifier: 10.1109/TPS.2018.2797120

The tokamak map trajectories can be obtained by directly integrating the field line differential equations, but the integration requires a time-consuming calculation which may not be appropriate for studying long-term of the field behavior. Therefore, approximated maps have to be considered if one wants to have the advantage of much shorter computation times [3], [10], [11]. Analytical tokamak maps can be derived from physical models and mathematical approximations applied to the field line equations, or even can be ad hoc maps to obtain a qualitative or quantitative description of the physical situation that they describe [11], [12], [13].

Magnetic field lines are, in general, orbits of Hamiltonian systems of one-and-a-half degrees of freedom with a time-like periodic coordinate. Consequently, the field line configuration can be represented in Poincaré sections at a fixed toroidal angle, equivalent to two-dimensional area-preserving maps [3], [10], [11]. Thus, we can use such maps to qualitatively represent the magnetic configurations of tokamak plasmas [14]. In this work, we present maps proposed to investigate the fundamental features of the magnetic field line dynamics in tokamaks with divertor. We introduce new versions of the Tokamap and Ullmann map for tokamaks with divertor and review the Divertor Map and an integrable map for equilibrium divertor configuration in toroidal geometry.

The paper is organized as follows: in Section II, we show the tokamak divertors. In Section III, we introduce three symplectic maps: the Divertor Map, the Tokamap for divertor configuration, and the Ullmann map for divertor. We also give examples of these maps to show their dynamical characteristics. In Section IV, we introduce an integrable map to simulate toroidal magnetic surfaces modified by a divertor. Section V contains the conclusions.

II. Divertor

In tokamaks, a material limiter separates the plasma column from the wall. However, to improve the plasma isolation and eliminate impurities, divertors have been used in several modern tokamaks and will be used in ITER [7]. Divertors consist of conductors arranged externally, that carry specific electric currents to create X point (or hyperbolic fixed point) where the poloidal magnetic field is null, due to the overlap of the magnetic fields of the conductors with the magnetic field of the plasma.

In Fig. (1), we present an example of the magnetic surfaces in a tokamak with divertor. In this figure, the separatrix in red, with one hyperbolic point, separates the internal toroidal magnetic surfaces with quasi-periodic lines of the external surfaces with open field lines. Moreover, from the X point arises a separatrix with two manifolds, one stable and the other unstable.

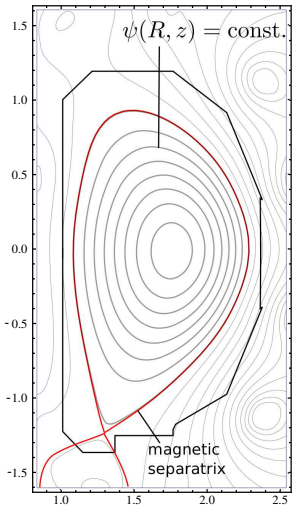

Fig. 1. (Color online) Schematic view of a tokamak divertor equilibrium configuration with intersection of invariant magnetic surfaces on a plane determined by a specific toroidal angle. The red line indicates the magnetic separatrix while the contours are magnetic surfaces.

Several tokamaks with divertors have nonaxisymmetric resonant perturbation coils designed specifically to modify the plasma magnetic field [1], [2]. One of the actions of the resonant perturbations created by these coils is to create chaotic magnetic field layers in the peripheral region of the plasma column [7], [11], [13].

In Fig. (2), we show an example of this kind of coils arranged around a tokamak chamber, similar to the coils used in DIII-D tokamak [15]. To show how the tokamak equilibrium is perturbed by the coils of Fig. (2), we present in Fig. (3), the transversal cross section of the diverted tokamak magnetic field lines for a set of control parameters commonly found in tokamak discharges [15], [16]. In Fig. (3) we can see chaotic lines and magnetic islands around the divertor hyperbolic point, the separatrix of the unperturbed diverted field, and the divertor plates where the chaotic lines intersect the tokamak chamber.

The chaotic layer at the plasma edge affects the plasma confinement [17] and can be controlled by the perturbation introduced by the divertor [7]. The chaotic layer in this region is mainly determined by the manifolds from the hyperbolic point [18].

III. Sympletic Maps

Symplectic maps have been commonly used in physics to describe Poincaré sections of dynamical systems [19], [20], [21]. In plasma physics, a pioneer symplectic map to describe particle orbits for stellarators was introduced in [22]. After that, symplectic maps have been used to investigate particle transport in magnetically confined plasmas [23], [24], [25]. Symplectic maps have also been introduced to investigate the chaotic field lines in tokamaks. The first one was the Martin-Taylor map introduced to describe the perturbation created by the ergodic magnetic limiter in tokamaks [26].

In this section, we present symplectic maps to describe the diverted magnetic field lines in tokamaks: the Divertor Map

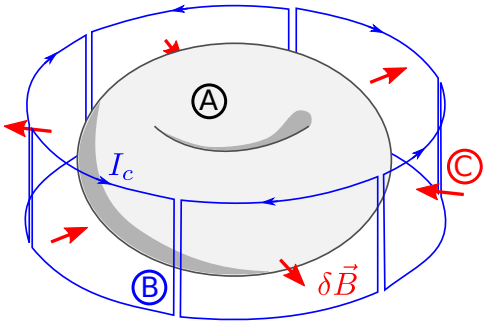

Fig. 2. (Color online) Schematic view of a tokamak vacuum chamber (A), and the external coils (B), responsible for the resonant magnetic field (C). Blue lines indicate the perturbing external currents and the red vectors the non-axisymmetric field perturbation.

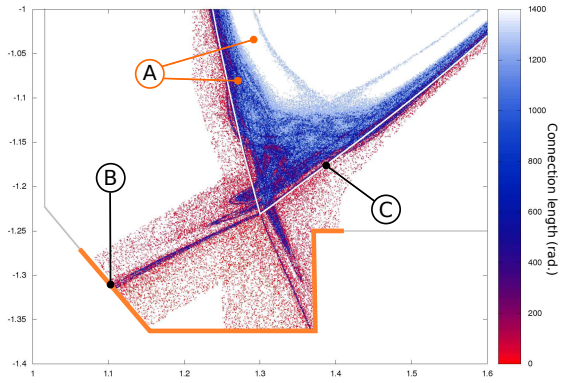

Fig. 3. (Color online) Detail of the Poincaré map of the perturbed field lines in the magnetic saddle region. The magnetic perturbation leads to the formation of a peripheral chaotic layer and magnetic islands (A). Chaotic field lines now cross the symmetric separatrix (C), and the open field lines intersect the tokamak chamber (B) in asymmetric patterns controlled by the invariant manifolds of the saddle.

introduced in [27] and new versions of the Tokamap [28] and the Ullmann's map [29] for divertors. These maps are nonintegrable and describe plasma equilibrium with chaotic layers, around the hyperbolic point, due to resonant perturbations.

A. Divertor Map

The first Divertor Map has been presented as the simplest model for the magnetic configuration of a tokamak equipped with a divertor. The map simulates Poincaré sections of field lines [27].

The Divertor Map introduced in [27] is

$$\begin{aligned} x_{n+1} &= x_n - k y_n (1 - y_n), \\ y_{n+1} &= y_n + k x_{n+1}, \end{aligned} \tag{1}$$

where (x_n, y_n) are the rectangular coordinates on the poloidal surface of section and the control parameter k determines both the safety factor and the strength of toroidal asymmetries in the magnetic field. In this map, the equilibrium and perturbation expressions can not be separated and, consequently, we can not describe the equilibrium without perturbation. For small values of the control parameter k, the map shows the formation of a thin chaotic layer in the separatrix region, whose chaotic orbits eventually reach the plates, which are set in the numerical

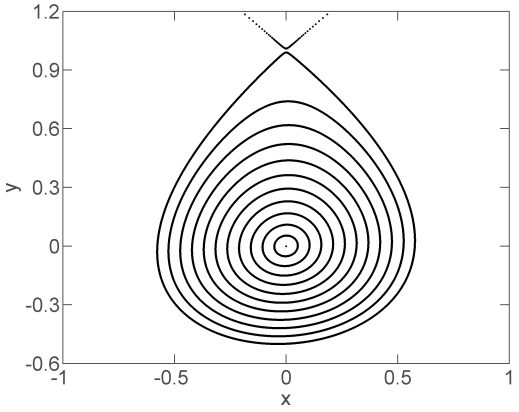

Fig. 4. Poincaré map of the Divertor Map for $k = 0.6$, depicting the stable fixed point at (0,0) and some invariant curves. Closed invariant lines are separated from open lines (not shown) by the separatrix, which includes the hyperbolic point at (0,1).

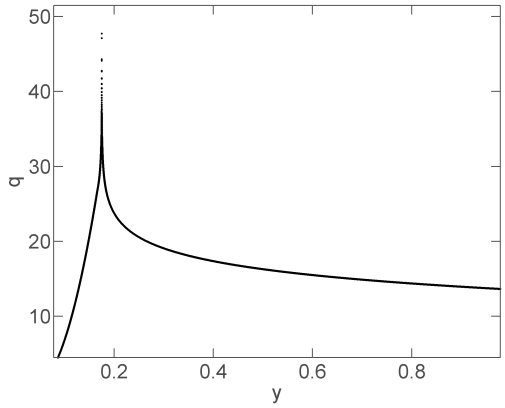

Fig. 5. Safety factor profile considered for the Tokamap to obtain Fig. (6). The coordinate y corresponds to the radial coordinate used in large aspect ratio tokamaks.

simulations at $y_{\rm plate} = 1$. One example is in Fig. (4) for $k = 0.6$.

B. Tokamap for Diverted Plasmas

The Tokamap has been introduced to describe field lines of a tokamak equilibrium modified by a resonant perturbation. There are several versions of this map to account for different equilibria and perturbations. Here, we consider the following version of the map for tokamak plasmas [28]:

$$\begin{aligned} \psi_{\rm k+1} &= \psi_{\rm k} - \frac{L}{2\pi}\frac{\psi_{\rm k+1}}{1+\psi_{\rm k+1}}\sin(2\pi\theta_{\rm k}), \qquad (2)\\ \theta_{\rm k+1} &= \theta_{\rm k} + \frac{1}{q(\psi_{\rm k+1})} - \frac{L}{2\pi}\frac{1}{(1+\psi_{\rm k+1})^2}\cos(2\pi\theta_{\rm k}), \end{aligned}$$

where L is a control parameter that simulates the resonant perturbation amplitude and q is the safety factor that characterizes the tokamak equilibrium.

We use rectangular coordinates $x = \frac{\theta}{2\pi}$, $y = 1 - \frac{\Psi}{\Psi_a}$, where $\Psi_a = \Psi$ at the plasma edge. We choose a safety profile divergent near the plasma edge ($x = 1$ at the plasma edge and $x = 0$ at the plasma centre). The considered profile is shown in Fig. (5). In Fig. (6), we show invariant and chaotic lines, around the hyperbolic point, for the control parameter $L = 0.1$. The observed chaotic layer appears in the resonant region.

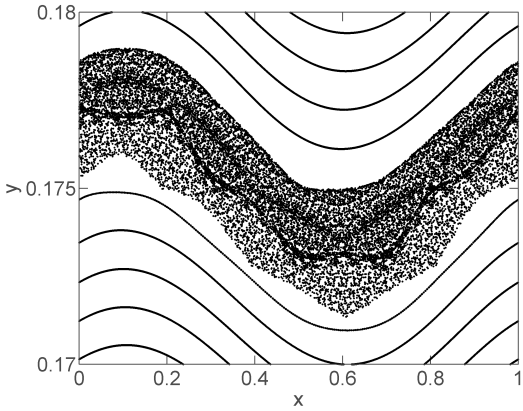

Fig. 6. Invariant magnetic surfaces and chaotic field lines obtained from the Tokamap for $L = 0.1$.

C. Ullmann Map for Diverted Plasma

A special set of coils, known as the ergodic limiter, have been proposed to create a chaotic layer at the tokamak plasma edge in order to separate the plasma from the wall [4]. Since then different kinds of limiters were installed in tokamaks to control the plasma confinement [12], [13], [30].

In [29] a symplectic map was proposed to describe tokamak field lines perturbed by an ergodic limiter. The map is valid for large aspect ratio tokamaks with toroidal correction. In this approximation, the toroidal coordinate is related to z. In the model, the topology of the magnetic field lines is described by a Poincaré map in the section $z = \text{constant}$, with variables $r_{\rm n}, \Theta_{\rm n}$ denoting the coordinates of the nth intersection of the field line on the considered section [12], [29].

The analytical expressions for the Poincaré map is obtained, for the equilibrium with toroidal correction, by the generating function:

$$\begin{aligned} G_{\rm TO}(r_{\rm n+1},\theta_{\rm n}) &= G_{\rm cil}(r_{\rm n+1},\theta_{\rm n}) \qquad (3)\\ &+ \sum_{\rm l=1}^{\infty} a_{\rm l}\left(\frac{r_{\rm n+1}}{R_0}\right)^{l}\cos(l\theta_{\rm n}), \end{aligned}$$

and the following relations:

$$r_{\rm n} = \frac{\partial G_{\rm TO}(r_{\rm n+1},\theta_{\rm n})}{\partial\theta_{\rm n}}, \qquad (4)$$

$$\theta_{\rm n+1} = \frac{\partial G_{\rm TO}(r_{\rm n+1},\theta_{\rm n})}{\partial r_{\rm n+1}}. \qquad (5)$$

where $G_{\rm cil}$ is the generating function corresponding to the cylindrical equilibrium. From equations (4) and (5) we obtain the map expressions

$$r_{\rm n+1} = \frac{r_{\rm n}}{1 - a_1\sin\theta_{\rm n}}, \qquad (6)$$

$$\theta_{\rm n+1} = \theta_{\rm n} + \frac{2\pi}{q(r_{\rm n+1})} + a_1\cos\theta_{\rm n}, \qquad (7)$$

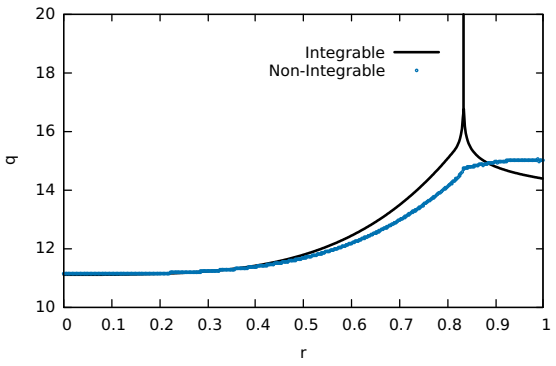

Fig. 7. Analytical safety factor profile, with a divergence near the plasma edge, and the safety factor profile calculated numerically, for a fixed θ. The coordinate r is normalized to a (plasma radius).

where a_1 is small and determined by the inverse of the tokamap aspect ratio, and $q(r)$ is the safety factor profile. The toroidal correction introduces a poloidal angle θ dependence on the map. Such correction, considered in the model, takes into account the outward magnetic surface displacement, characteristic of tokamak equilibrium in toroidal geometry. The constant $a_1 = -0.04$ was fit to reproduce the observed tokamak magnetic surface displacements [29]. Since the map is derived from a generating function, interpreted as a canonical transformation between the previous and the next coordinates, the Jacobian for this map is unitary and, consequently, the map is symplectic [12], [29].

We consider the Ullmann map with the safety factor profile used in the tokamap without the toroidal corrections, i.e. $a_1 = 0$, which is integrable. This is compared with the safety factor profile of the non-integrable case with toroidal correction $a_1 = -0.04$. The latter must be obtained numerically by inverting the rotation number of an appropriate collection of initial conditions. This is accomplished using the relation

$$q = \frac{1}{l} \rightarrow q \equiv \lim_{k\to\infty} \frac{2\pi k}{\sum_{j=0}^{k}(\theta_{j+1} - \theta_j)}. \tag{8}$$

In Fig. (7), we have the analytical safety factor profile obtained from this definition and, for initial conditions with a fixed θ, the modified safety factor calculated numerically for 100 values of r between 0 and 1. We see in Fig. (7) the difference between the original profile inserted in equation (7) and the one calculated, considering the toroidal correction, by applying equation (8). The profiles are the same in the plasma centre and differ at the plasma edge. As shown in [12] and [29], we can add another symplectic map as an external perturbation to obtain a chaotic layer on the resonant region.

IV. Integrable Map for toroidal Magnetic Surfaces

In this section, we introduce a procedure to obtain an integrable map simulating a plasma equilibrium for a diverted tokamak [31], [32], [33].

To obtain the desired map it is necessary, initially, to find a potential $V(y)$ that produces a topology with an X-point, with a Hamiltonian ψ given by

$$\psi = \frac{x^2}{2} + V(y). \tag{9}$$

In the plasma map this Hamiltonian will be the flux function. We choose a double-well shaped potential to create curves in phase space that exhibit two closed regions delimited by a separatrix between them with an X point. The expression for $V(y)$ with the desired properties will be written as a set of six parabolas, indicated in Fig. (8a), joined smoothly the connection points. In Fig (8a) each portion between two dashed lines has its own parameters, then there are six different parabolas joining smoothly at the dashed lines. Figure (8a) shows the chosen potential profile used in this article [31]. A higher number of parabolas could be used to adapt the plasma shape to a desired boundary. Three parabolas is the minimum to reproduce the divertor configuration with one hyperbolic and two elliptic points. The position $y = 0$ corresponds to the plasma center. In Fig. (8b), we present the separatrix for the orbits obtained for the chosen potential of Fig. (8a). This separatrix determines, in the map, the last closed magnetic surfaces inside the plasma.

We choose an analytical expression for the potential represented in Fig. (8a). For this potential, the trajectory corresponding to the separatrix is shown in Fig. (8b), for ITER parameters.

The next step is to solve Hamilton's equations to get x and y in terms of their initial conditions (x_0, y_0) and time t,

$$\frac{dx}{dt} = -\frac{\partial\psi}{\partial y}, \tag{10}$$

$$\frac{dy}{dt} = \frac{\partial\psi}{\partial x}. \tag{11}$$

The continuous equations are transformed into a discrete map, where the continuous time parameter t is turned into a discrete time step Δ:

$$x(x_0, y_0, t) = x_{n+1}(x_n, y_n, \Delta), \tag{12}$$

$$y(x_0, y_0, t) = y_{n+1}(x_n, y_n, \Delta). \tag{13}$$

To obtain the magnetic surfaces we choose Δ given by the inverse of the safety factor

$$\Delta = \frac{T(\psi)}{q(\psi)}. \tag{14}$$

where $T(\psi)$ is the rotation period of the invariant curves associated with the continuous system and $q(\psi)$ is the safety factor of the magnetic surface we intend to represent by the invariant curve [31], [33].

We choose a monotonic safety factor profile similar to the one used before in Section III (B) and (C) expressed in terms of the function ψ [31]:

$$q(\psi) = \begin{cases} q_0 + c_1\psi + c_2\psi^2, & \psi \le \psi_{95}, \\ \alpha\ln(\psi_S - \psi) + \beta, & \psi > \psi_{95}. \end{cases}$$

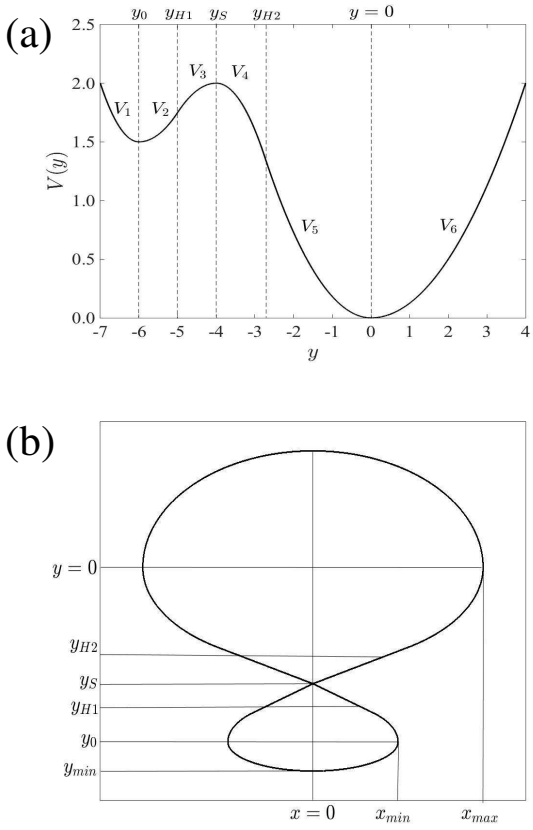

Fig. 8. (a) Potential used to obtain the magnetic surfaces. (b) Schematic view of a separatrix in rectangular coordinates indicating the meaning of each geometric parameter related to $V(y)$ for the normalized geometric parameters $x_{\rm max}=-2$, $x_{\rm min}=-1$, $y_{min}=7$, $y_{\rm max}=4$, $y_{\rm H1}=5$, $y_{\rm H2}=2.75$, $y_{\rm S}=4$, $y_0=6$.

In the numerical examples we choose the safety factor parameters such that the equilibrium magnetic shear at the reference surface, defined as

$$\hat{s}_{95}=\frac{r_{95}}{q_{95}}\frac{dq}{dr}\Big|_{\rm r_{95}}, \tag{15}$$

are $\hat{s}_{95}=110.8$ and $q_{95}=3.3$.

For each line, the value of ψ is given by $\psi=\psi(x_0,y_0)$. At each point (x_0,y_0), ψ determines the Δ value:

$$\Delta=\Delta(\psi). \tag{16}$$

The map gives the Poincaré map on the surface $\varphi=0$

$$M_\Delta(x_{\rm n},y_{\rm n})=(x_{\rm n+1},y_{\rm n+1}). \tag{17}$$

The magnetic surfaces are shown in Fig. (9).

To perturb the divertor integrable map, we apply the symplectic Martin-Taylor map [26], that simulates the effect of an ergodic limiter in large aspect-ratio tokamaks, which introduces external symmetry-breaking resonances, to generate a chaotic region near the separatrix passing through the X-point.

For each toroidal turn, the Martin Taylor map is applied at the $\varphi=0$ surface as a kick perturbation:

$$(x^*,y^*)=M_{\Delta_{\rm n}}(x_{\rm n},y_{\rm n}), \tag{18}$$

$$(x_{\rm n+1},y_{\rm n+1})=P(x^*,y^*). \tag{19}$$

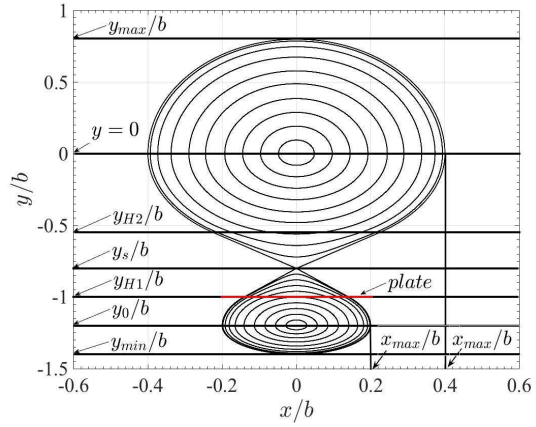

Fig. 9. (Color online) Invariant magnetic surfaces obtained from the integrable map for the chosen parameters indicated in the text.

Thus, the map used to describe the perturbation of an external resonant helical perturbation due to a magnetic limiter is given by [26]

$$x_{\rm n+1} = x_{\rm n}-me^{-\frac{my_{\rm n}}{r_{\rm m}}}\cos\left(\frac{mx_{\rm n}}{r_{\rm m}}\right), \tag{20}$$

$$y_{\rm n+1} = y_{\rm n}+\frac{r_{\rm m}}{m}\log\left\{\cos\left[\frac{mx_{\rm n}}{r_{\rm m}}-me^{-\frac{mx_{\rm n}}{r_{\rm m}}}\cos\left(\frac{mx_{\rm n}}{r_{\rm m}}\right)\right]\right\} - \frac{r_{\rm m}}{m}\log\left\{\cos\left(\frac{mx_{\rm n}}{r_{\rm m}}\right)\right\}, \tag{21}$$

where the parameter m quantifies the perturbation strength, proportional to the current in the limiter coils, s is the magnetic shear at the plasma edge, and $r_{\rm m}$ is the plasma radius. The composed field line map is used to obtain the perturbed field line configurations, shown in Fig. (10), with different magnetic shear profiles at the plasma edge for the control parameters $s=1.9$ and $s=2.5$ for $m=3$. The current in the ergodic limiter is the same in Figs. (10a) and (10b) .

The introduced non-axisymmetric stationary magnetic perturbation leads to the formation of homoclinic tangles near the divertor magnetic saddle [18]. These tangles intersect the divertor plates in static helical structures.

In Fig. (10), we see that the size of the chaotic area near the hyperbolic point depends on the magnetic shear. This dependence is shown in Fig. (11) where we present the chaotic width, the distance from the hyperbolic point to the border of the chaotic region (computed at $y=y_{\rm s}$) as a function of the parameter s in the interval $1.5<s<2.8$, for two different m values. The chaotic area increase should correspond to higher average diffusion time for magnetic field lines to cross the chaotic region. The width increase is not monotonic due to a series of bifurcations that occurs for increasing shear.

V. Conclusions

To describe Poincaré sections of diverted magnetic field lines, we presented two-dimensional symplectic maps, in the limit of large aspect ratio simulating the alterations the magnetic topology caused by the divertor.

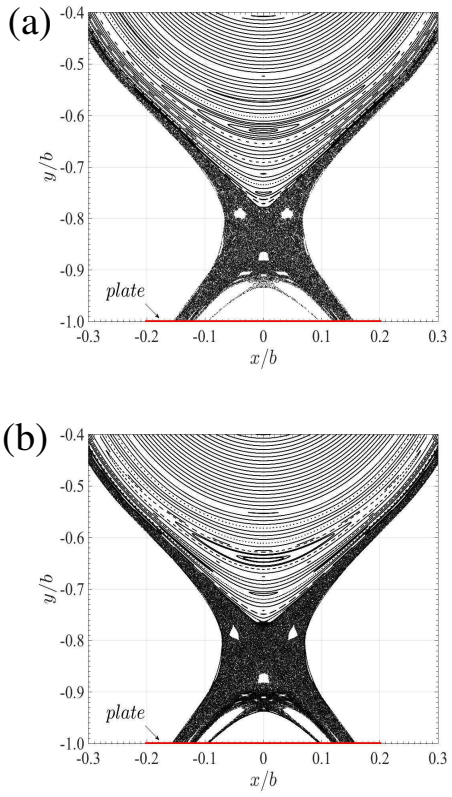

Fig. 10. (Color online) Phase portrait for the total field line map. (a) $s = 1.9$ and $m = 3$, (b) $s = 2.5$ and $m = 3$.

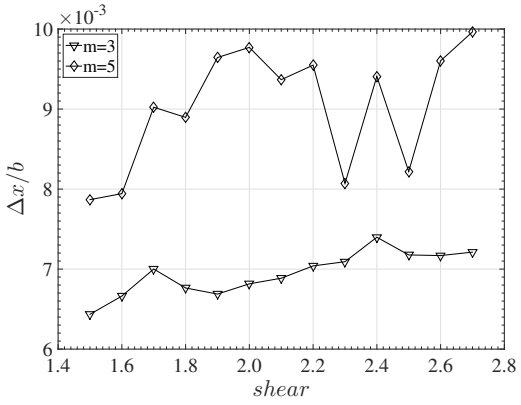

Fig. 11. Normalized width of chaotic area as a function of the magnetic shear s, for $m = 3$ and $m = 5$ and the same parameters of Fig. (10).

These maps can be used to investigate the main characteristics of the chaotic layer around the hyperbolic point introduced by divertors, and how these characteristics change with the equilibrium and perturbation control parameters. The Tokamap and Ullmann map were presented in new versions for tokamaks with divertor. We also presented a map describing magnetic surfaces in toroidal geometry.

All the maps introduced in this article are useful for studying different aspects of the field line dynamics and transport in tokamaks with divertor. Extensions of the presented maps could be derived to include additional effects not considered in this article, such as the particle's finite Larmor radius [34], [35] and the screening caused by the plasma response to resonant magnetic perturbations [36], [37].

ACKNOWLEDGMENT

This work was partially supported by the National Council for Scientific and Technological Development (CNPq) – Brazil, grants $870198/1997-1$ and $830577/1999-8$ and the São Paulo Research Foundation (FAPESP) grants $2012/18073-1$, $2015/07311-7$ and $2011/19296-1$. PJM was supported by the U.S. Department of Energy Contract No.DE – FG05 – 80ET – 53088.

REFERENCES

[1] C. W. Horton, Jr. S. Benkadda, *ITER Physics*, 1nd ed., Singapore, MY: World Scientific Publishing, 2015, pp. 248.
[2] C. W. Horton, *Turbulent Transport in Magnetized Plasmas*, 1nd ed., New Jersey, USA: World Scientific Publishing, 2012, pp. 520.
[3] R. D. Hazeltine, J. D. Meiss, *Plasma Confinement*, 1nd ed., New York, USA: Dover Books on Physics, 2003, pp. 480.
[4] F. Karger, K. Lackner, "Resonant helical divertor," *Phys. Lett. A*, vol. 61, pp. 385-387, Jun. 1977.
[5] F. Wagner, G. Becker, K. Behringer, D. Campbell, A. Eberhagen, W. Engelhardt, G. Fussmann, O. Gehre, J. Gernhardt, G. V. Gierke, G. Haas, M. Huang, F. Karger, M. Keilhacker, O. Klüber, M. Kornherr, K. Lackner, G. Lisitano, G. G. Lister, H. M. Mayer, D. Meisel, E. R. Müller, H. Murmann, H. Niedermeyer, W. Poschenrieder, H. Rapp, H. Röhr, F. Schneider, G. Siller, E. Speth, A. Stäbler, K. H. Steuer, G. Venus, O. Vollmer, and Z. Yü, "Regime of Improved Confinement and High Beta in Neutral-Beam-Heated Divertor Discharges of the ASDEX Tokamak," *Phys. Rev. Lett.*, vol. 49, no. 19, pp. 1408-1414, Nov. 1982.
[6] M. Kikuchi, K. Lackner, M. Q. Tran, *Fusion Physics*, 1nd ed., Vienna, AT: IAEA, 2012, pp. 1129.
[7] ITER Physics Expert Group on Divertor, "Power and Particle Control," *Nucl. Fusion*, 1999, ch. 4, vol. 39, pp. 2391-2469.
[8] T. E. Evans, R. A. Moyer, and P. Monat, "Modeling of stochastic magnetic flux loss from the edge of a poloidally diverted tokamak," *Phys. Plasmas*, vol. 9, pp. 4957-4967, Nov. 2002.
[9] E. C. da Silva, I. L. Caldas, R. L. Viana, and M. A. F. Sanjuán, "Escape patterns, magnetic footprints, and homoclinic tangles due to ergodic magnetic limiters," *Phys. Plasmas*, vol. 9, pp. 4917-4928, Nov. 2002.
[10] P. J. Morrison, "Magnetic Field Lines, Hamiltonian Dynamics, and Nontwist Systems," *Phys. Plasmas.*, vol. 7, pp. 2279-2289, May. 2000.
[11] S. S. Abdullaev, *Construction of Mappings for Hamiltonian Systems and Their Applications*, 2nd ed., Berlin: Springer-Verlag Berlin Heidelberg, vol. 691, 2006, pp. 379.
[12] J. S. E. Portela, I. L. Caldas, R. L. Viana, "Tokamak magnetic field lines described by simple maps," *Eur. Phys. J. Spec. Top.*, vol. 165, pp. 195-210, Dec. 2008.
[13] I. L. Caldas, R. L. Viana, M. S. T. Araujo, A. Vannucci, E. C. da Silva, K. Ullmann, M. V. A. P. Heller, "Control of Chaotic Magnetic Fields in Tokamaks," *Braz. J. Phys.*, vol. 32, no. 4, pp. 980-1004, Dec. 2002.
[14] S. R. Barocio, E. Chávez-Alarcón, C. Gutierrez-Tapia, "Mapping the intrinsic stochasticity of tokamak divertor configuration," *Braz. J. Phys.*, vol. 36, no. 2B, pp. 550-556, Jun. 2006.
[15] D. Ciro, T. E. Evans, I. L. Caldas, "Modeling non-stationary, non-axisymmetric heat patterns in DIII-D tokamak," *Nucl. Fusion*, vol. 57, no.016017, 2017.
[16] C. G. L. Martins , M. Roberto , I. L. Caldas. "Delineating the magnetic field line escape pattern and stickiness in a poloidally diverted tokamak," *Physics of Plasmas*, vol. 21, no. 082506, Jul. 2014.
[17] A. Vannucci, I. L. Caldas, I. C. Nascimento, "Disruptive instabilities in the discharges of the TBR-1 small Tokamak," *Plas. Phys. Control. Fusion*, vol. 31, pp. 147, Feb. 1989.
[18] A. Wingen, T. E. Evans, and K. H. Spatschek, "High resolution numerical studies of separatrix splitting due to non-axisymmetric perturbation in DIII-D," *Nucl. Fusion*, vol. 49, no. 5, pp. 055027, Apr. 2009.
[19] J. D. Meiss, "Symplectic maps, variational principles, and transport," *Rev. Mod. Phys.*, vol. 64, no. 3, pp. 795-848, Jul. 1992.
[20] J. M. Greene, "A method for determining a stochastic transition," *J. Math. Phys.*, vol. 20, no. 6, pp. 1183-1201, Jun. 1979.

[21] B. V. Chirikov, "A universal instability of many-dimensional oscillator systems," *Phys. Rep.*, vol. 52, no. 5, pp. 263-379, May. 1979.
[22] M D. Kruskal, "Some properties of rotational transforms," *AEC Report*, Springfield: VA, 1952, no. NYO-998, PM-S-5.
[23] W. Horton, H-B. Park, J-M. Kwon, D. Strozzi, P. J. Morrison, D-I, Choi, "Drift wave test particle transport in reversed shear profile," *Phys. Plasmas*, vol. 5, no. 11, pp. 3910-3917, Nov. 1998.
[24] D. del Castillo-Negrete, P.J. Morrison, "Chaotic transport by Rossby waves in shear flow," *Phys. Fluids A*, vol. 5, no. 4, pp. 948-965, Apr. 1993.
[25] D. del Castillo-Negrete, J. Greene, P.J. Morrison, "Area preserving nontwist maps: periodic orbits and transition to chaos," *Physica D*, vol. 91, pp. 1-23, Mar. 1996.
[26] T. J. Martin and J. B. Taylor. "Ergodic behaviour in a magnetic limiter," *Plas. Phys. Control. Fusion*, vol. 26, pp. 321-340, Mar. 1984.
[27] A. Punjabi, A. Verma, A. Boozer, "Stochastic broadening of the separatrix of a tokamak divertor," *Phys. Rev. Lett.*, vol. 69, no. 23, pp. 3322-3325, Dec. 1992.
[28] R. Balescu, M. Vlad, F. Spineanu, "Tokamap:A Hamiltonian twist map for magnetic field lines in a toroidal geometry," *Phys. Rev. E.*, vol. 58, pp. 951-964, Jul. 1998.
[29] K. Ullmann, I.L. Caldas, "A symplectic mapping for the ergodic magnetic limiter and its dynamical analysis," *Chaos, Solitons and Fractals*, vol. 11, no. 13, pp. 2129-2140, Oct. 2000.
[30] Ph. Ghendrih, A. Grosman, and H. Capes, "Theoretical and experimental investigations of stochastic boundaries in tokamaks," *Plas. Phys. Control. Fusion*, vol. 38, no. 10, pp. 1653-1724, 1996.
[31] T. Kroetz, M. Roberto, I. L. Caldas, R. L. Viana, P. J. Morrison, "Divertor map with freedom of geometry and safety factor profile," *Plas. Phys. Control. Fusion*, vol. 54, no. 4, pp. 045007, Mar. 2012.
[32] T. Kroetz, M. Roberto, I. L. Caldas, R. L. Viana, P. J. Morrison, P. Abbamonte, "Integrable maps with non-trivial topology: application to divertor configurations," *Nucl. Fusion*, vol. 51, no. 034003, Feb. 2010.
[33] G. Roberson, M. Roberto, I. L. Caldas, T. Kroetz, R. L. Viana. "Shaping Diverted Plasmas With Symplectic Maps," *IEEE Transactions on Plasma Physics*, vol. 45, no. 3, pp. 356-363, Feb. 2017.
[34] J. J. Martinell and D. del-Castillo-Negrete, "Gyroaverage effects on chaotic transport by drift waves in zonal flows," *Phys. Plasmas*, vol. 20, no. 022303, Feb. 2013.
[35] J. D. da Fonseca, D. del-Castillo-Negrete, and I. L. Caldas. "Area-preserving maps models of gyroaveraged ExB chaotic transport," *Phys. Plasmas*, vol. 21, no. 092310, Sep. 2014.
[36] A. Wingen, N. M. Ferraro, M. W. Shafer, E. A. Unterbeg, J. M. Canik, T. E. Evans, D. L. Hillis, S. P. Hirshman, S. K. Seal, P. B. Snyder, and A. C. Sontag, "Connection between plasma response and resonant magnetic perturbation (RMP) edge localized mode (ELM) suppression in DIII-D," *Plasma Phys. Control. Fusion*, vol. 57, no. 10, p. 104006, Sep. 2015.
[37] A. C. Fraile Jr, M. Roberto, I. L. Caldas and Caroline G. L. Martins, "Plasma Response to Resonant Magnetic Perturbations in Large Aspect Ratio Tokamaks," *IEEE Trans. Plas. Scien.*, vol. PP, pp. 1-7, no. 99, Oct. 2017.

Iberê Luiz Caldas Iberê was born in Santos, Brazil, in 1948. He received the B.S. and Ph.D. degrees in physics from the Institute of Physics of University of São Paulo (IF-USP), São Paulo, Brazil, in 1970 and 1979, respectively. In 1977-1979, 1983, 1984, and 1988, he was a Guest Scientist with the Max-Planck-Institut für Plasmaphysik, Garching bei München, Germany. Since 1995, he has been a Full Professor with IF-USP. His current research interests include plasma physics and chaos.

Bruno Bartoloni Bruno received the Ph.D. degree in plasma physics from the Institute of Physics, Universidade de São Paulo, Brazil, in 2016. His research involved different current density profiles applied in symplectic maps to study the magnetic field lines in a plasma confined in a tokamak. He has been a Professor with the Physics Department, Faculdade de Tecnologia de São Paulo, since 2017.

David Ciro D. Ciro received his B.S. degree in Physics from the Antioquia University in 2010 (Colombia), M.Sc and Ph.D degrees in Physics from the São Paulo University in 2012 and 2016 (Brazil). In 2015 he was a visiting researcher in the DIII-D facilities, General Atomics (CA, USA). Currently, he develops his Post-Doctoral research at the Institute of Physics - São Paulo University, in Non-linear Dynamics applied to Plasma Physics.

Geraldo Roberson Geraldo received the B.Sc. degree in physics from the Federal University of Pernambuco, Recife, Brazil, and the M.Sc. degree in plasma physics from the Technological Institute of Aeronautics, São José dos Campos, Brazil, where he is currently pursuing the Ph.D. degree in sciences and space technologies.

Adriane Schelin Adriane received the Ph.D. degree in physics from the Institute of Physics, University of São Paulo, Brazil, in 2009. From 2009 to 2010, she was a visiting researcher with the Heinrich-Heine-Universität Düsseldorf, Germany. In 2011 and 2012, she was a professor at the Physics Academic Department, Universidade Tecnológica Federal do Paraná, Curitiba, Brazil. She has been a Professor with the Institute of Physics, University of Brasilia, Brazil, since 2013.

Tiago Kroetz Tiago received the Ph.D. degree in plasma physics from the Instituto Tecnolgico de Aeronáutica, São José dos Campos, Brazil, in 2010. Since 2010, he has been involved in research about nonlinear dynamics applied to plasma physics and mechanical systems, and also extended to the field of research on the physics education. He has been a Professor with the Physics Academic Department, Universidade Tecnológica Federal do Paraná, Pato Branco, Brazil, since 2012.

Marisa Roberto Marisa received the B.S. degree in physics from the Catholic University of São Paulo, São Paulo, Brazil, in 1982, the M.S. degree from the Space Research Institute, São José dos Campos, Brazil, in 1986, and the Ph.D. degree in plasma physics from the Aeronautic Institute of Technology (ITA), in São José dos Campos, in 1992. In 1999 and 2004, she was a Visiting Scholar with the University of California at Berkeley, Berkeley, CA, USA. She is currently a Full Professor with the Physics Department, ITA. Her current research interests include plasma physics for technological applications and chaos.

Ricardo Luiz Viana Ricardo Viana received the Ph.D. degree in plasma physics from the Institute of Physics, Universidade de São Paulo, Brazil, in 1991. In 1987, he was a Visiting Scholar with the Institute for Physical Science and Technology, University of Maryland, College Park, MD, USA. He has been a Professor with the Physics Department, Universidade Federal do Paraná Curitiba, Curitiba, Brazil, since 1989. He has authored 190 papers and supervised ten doctoral theses, and three post-doctoral works.

Kelly Cristiane Iarosz Kelly received the Ph.D. degree in Science/Physics from the State University of Ponta Grossa, Paraná, Brazil, in 2013. In 2014, she was a visiting researcher with the Institute for Complex Systems and Mathematical Biology at Aberdeen University (honorary researcher since 2015). In 2017, she was a academic visiting with the Complex Systems and Control at Xi'an University of Tecnology, China. In 2108, she is visiting researcher with Humboldt-Universität zu Berlin and Potsdam Institute for Climate Impact Research, Germany.

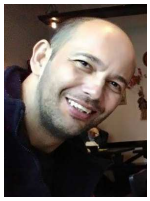

Antonio Marcos Batista Antonio received the Ph.D. degree in Physics from the Federal University of Paraná in 2001. From 2014 to 2015, he was a visiting researcher with the Institute for Complex Systems and Mathematical Biology at Aberdeen University (honorary researcher since 2015). He was visiting Scholar in Potsdam Institute for Climate Impact Research (2016) and Xi'an University of Tecnology (2017). He is currently an Associate professor in Matematics and Statistics Department at State University of Ponta Grossa since 1997.

Philip J. Morrison Philip is mathematical and theoretical physicist with broad interests. As a member of the Institute for Fusion Studies, he has worked on basic and applied plasma physics problems. He has been associated with the Geophysical Fluid Dynamics Program for twenty years, and as a member of its faculty work on basic and applied fluid mechanics problems. He has investigated the nonlinear Hamiltonian dynamics of few and infinite degree-of-freedom systems for many years. He has also worked on developing and applying advanced computational algorithms, in part through affiliation with the ICES Applied Mathematics Group.